



Chest X-Ray as the First Pointer in Various Skeletal Dysplasia and Related Disorders

Rupali Jain¹ Priyanka Naranje¹ Neerja Gupta² Pallavi Sinha¹ Madhulika Kabra²
Arun Kumar Gupta¹ Manisha Jana¹

¹Department of Radiology, All India Institute of Medical Sciences, Ansari Nagar, New Delhi, India

²Department of Pediatrics, All India Institute of Medical Sciences, Ansari Nagar, New Delhi, India

Address for correspondence Dr. Manisha Jana, MD, DNB, FRCR, Room No. 81C, Department of Radiodiagnosis, All India Institute of Medical Sciences, Ansari Nagar, New Delhi, India (e-mail: manishajana@gmail.com).

Indographics 2022;1:196–207.

Abstract

Keywords

- radiograph
- CXR
- dysplasia
- mucopolysaccharidosis
- spondylocostal dysostosis

Chest X-ray (CXR) is the most commonly used imaging modality. It is commonly used for respiratory or cardiac ailments; however, it is also used routinely as a part of skeletal surveys. In the case of suspected skeletal dysplasia, the viewer is alerted regarding the presence of some skeletal abnormality. But in case of a routine CXR performed for some other reason, it is not uncommon to miss subtle pointers of skeletal dysplasia. Sometimes routine CXR is the first pointer to alert a radiologist toward some generalized skeletal anomaly and therefore, initiate its proper evaluation by the skeletal survey.

Introduction

Skeletal dysplasia comprises a group of disorders involving abnormalities in the bones and cartilages. According to the current nosology of skeletal dysplasias,¹ there are 461 diseases and 42 classes of disorders. The skeletal survey is the most important radiological investigation in the assessment of dysplasias. Chest X-ray (CXR) forms an integral part of the skeletal survey. While assessing chest radiographs, a systematic approach is to be followed. Chest radiographs can reveal characteristic findings in the bones (including clavicles, ribs, vertebrae, sternum, scapula, humeral head) in a large number of skeletal dysplasias. In an unsuspected case, CXR can even provide the first diagnostic clue to

skeletal dysplasia. This article will review the chest radiograph findings in various common and clinically important skeletal dysplasias.

Imaging Features in Specific Skeletal Dysplasias

Since a detailed discussion of all dysplasias is beyond the scope of this article, we shall have an imaging feature-based discussion, based on the information a chest radiograph (► Fig. 1) can provide.

An assessment of the bone density should be the first step. A generalized decrease in bone density points toward a metabolic bone disease or a specific group of bone dysplasia

DOI <https://doi.org/10.1055/s-0042-1759845>.

© 2022. Indographics. All rights reserved.

This is an open access article published by Thieme under the terms of the Creative Commons Attribution-NonDerivative-NonCommercial-License, permitting copying and reproduction so long as the original work is given appropriate credit. Contents may not be used for commercial purposes, or adapted, remixed, transformed or built upon. (<https://creativecommons.org/licenses/by-nc-nd/4.0/>)

Thieme Medical and Scientific Publishers Pvt. Ltd., A-12, 2nd Floor, Sector 2, Noida-201301 UP, India

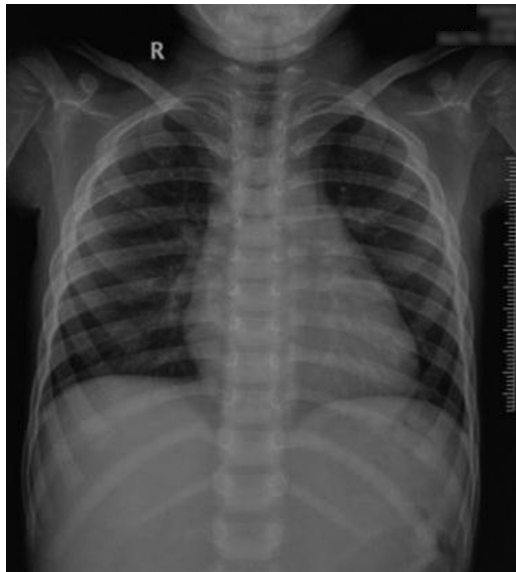


Fig. 1 Normal. Normal chest radiograph of a 12 year old boy.

(e.g., osteogenesis imperfecta). On the contrary, an increased bone density can be indicative of sclerosing bone dysplasia, besides other diagnostic considerations.

Normal Bone Density

Abnormality in the Ribs

Mucopolysaccharidoses (MPS): Defect in mucopolysaccharide degradation pathway leads to its progressive accumulation in the body, predominantly in central nervous system, bones, and heart.

Prominent imaging finding on a chest radiograph (CXR) includes paddle shaped/spatulated appearance of ribs (**► Fig. 2**). Inferior beaking of vertebrae in MPS type I and central beaking in MPS type 4 is evident on a lateral radiograph.² Other imaging findings include platyspondyly and widening of disk spaces, varus deformity of humerus with mildly hypoplastic epiphysis and proximal humeral notching, small scapula with glenoid cavities flattening, and thick and short clavicles.² Other characteristic imaging findings are discussed in **► Table 1**.²

Mucopolipidoses: This group of disorders has overlapping imaging features with MPS. Apart from paddle-shaped ribs in CXR, other indicative findings include undermodeling of the long bones (humeri), and periosteal “cloaking” in long bones

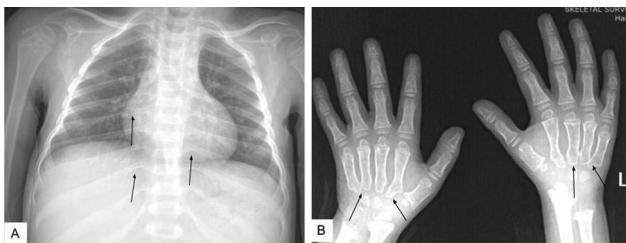


Fig. 2 (A,B) Mucopolysaccharidosis. CXR (A) shows paddle shaped ribs (arrows), tapered posteriorly and widened laterally, hand radiograph (B) shows proximal pointing of metacarpals (arrows)

(**► Fig. 3**). The latter feature is more evident in infancy and decreases thereafter.³

Pseudoachondroplasia: This is a type of spondyloepiphyseal dysplasia presenting as rhizomelic dwarfism, resulting from a mutation in *COMP* gene. On a frontal CXR, the striking imaging finding is the prominence and widening of posterior costo-chondral and costovertebral junctions⁴ (**► Fig. 4**). Other features in CXR include irregular and fragmented humeral epiphysis and metaphyseal flaring. Characteristic vertebral changes are evident on a lateral radiograph and include platyspondyly and anterior tongue-like projections.⁴ Other imaging findings in the skeletal survey are listed in **► Table 1**.⁴

Hereditary multiple exostoses: It is caused by an abnormality in bone remodeling of epiphyseal growth plate cartilage. CXR may show bony outgrowth having continuity with underlying ribs⁵ (sessile form may not be very apparent; **► Fig. 5**). Similar exostoses may be evident on other visible bones as well.

Encondromatosis: In this disorder, multiple enchondromas are associated with faulty cartilaginous development and abnormal formation of intraosseous cartilaginous foci. Enchondromas may be seen on CXR as expansile lytic rib lesions, with/without ring or arc-like calcific foci within⁶ (**► Fig. 6**). When no calcific focus is apparent, it closely mimics fibrous dysplasia.

Fibrous dysplasia: It is characterized by the localized developmental defect of osteoblast with its replacement by fibrous tissue and immature woven bone. On CXR, the lesions are seen as smooth expansile lytic ground glass lesion with “rind sign”⁷ (**► Fig. 7**). Polyostotic fibrous dysplasia may be associated with deformity of the long bones as well.

Spondylocostal dysostosis: Various types of spondylocostal dysostosis are described. The rib anomalies on CXR include absence, abnormal fusion, abnormal bifid ribs, etc., always associated with variable segmentation anomalies involving ≥ 10 thoracic vertebrae⁸ (**► Fig. 8**).

Nonaccidental injury: Its hallmark is evidence of repeated injury clinically and radiologically as a consequence of child abuse in infants/young children. Sinister findings include multiple posterior rib fractures of different ages.⁹ Other imaging clues on a CXR include scapular fracture (**► Fig. 9**), sternal fracture (difficult to detect on CXR), and the classic metaphyseal lesion or bucket-handle type of fracture involving the proximal/ distal humeri⁹. Other imaging findings are enlisted in **► Table 1**.⁹

Dysplasias with short ribs: Normally, the anterior ends of the true ribs are seen anteriorly for about half the hemithoracic diameter. When the ribs are not seen in the anterior part/stops right after the lateral ends, a short-rib dysplasia may be looked for. Important entities in this group are short-rib polydactyly syndromes (SRPS), Jeune's asphyxiating thoracic dystrophy (JATD), and Ellis Van Creveld syndrome (EVC). On a molecular basis, they all fall in the spectrum of ciliary disorders (ciliopathy).¹⁰ CXR gives a clue to diagnosis; however, imaging differentiation between them is not always possible based on a CXR alone and may need a complete skeletal survey. SRPS has polydactyly and a small narrow thorax with short ribs.¹⁰ JATD shows a typical narrow “bell-shaped” thorax and elevated “handle-bar” clavicles¹¹ (**► Fig. 10**). EVC clinically presents

Table 1 Key imaging features of various skeletal dysplasias where CXR shows diagnostic findings

Disease entity	Findings in CXR	Findings in other radiographs
Mucopolysaccharidoses	Paddle shaped/spatulated appearance of ribs (tapered posteriorly and widened anteriorly) Thick and short clavicles Thoracolumbar kyphosis/gibbus Vertebral bodies malformation <ul style="list-style-type: none"> • Inferior beaking (middle beaking in morquio) • Posterior scalloping Varus deformity of humerus with mildly hypoplastic epiphysis Proximal humeral notching Short sternum Small scapula with glenoid cavities flattening	Macrocephaly Thickening of cortical bone Abnormal J- shaped sella turcica Lack of pneumatization of paranasal sinuses Obtuse mandibular angle Prognathism Atlantoaxial instability Cervical kyphosis Anteroinferior/ central beaking Anisospondyly Rounded iliac wings Inferior tapering of ilium, Hip dysplasia Poorly developed acetabulum Underdeveloped proximal femoral epiphysis Coxa valgus Genu valgum Irregular hypoplastic tarsal and carpal bones Proximally pointed metatarsals and metacarpals Bullet shaped phalanges
Pseudoachondroplasia	Costo-transverse and costo- chondral junction widening Shortening of long bones (proximal > distal) Irregular and fragmented epiphysis Metaphyseal flaring Central anterior tongue appearance (pathognomic): Anterior part of vertebral body has tongue like protrusion (in lateral radiograph) Platypondyly : At older age Disc space widening	Odontoid dysplasia Squared pelvis with broad iliac wings Narrow sacrosciatic notch Poorly formed acetabulum with horizontal roofs Shortening of long bones (proximal > distal) Irregular and fragmented epiphysis Metaphyseal flaring Medial beaking of femoral neck (characteristic) Skull, facial bones and interpeduncular distance are normal (vs achondroplasia)
Non accidental injury	Multiple rib fractures, posterior especially Classic metaphyseal lesions- bucket handle, corner fracture (humerus) Sternal fractures Scapular fractures Spinous process fractures Clavicular fractures Spiral and oblique fractures of humerus Epiphyseal fractures Vertebral body fractures Note: Fractures of different ages are highly suspicious	Complex and linear skull fracture Classic metaphyseal lesions- (bucket handle, corner fracture other long bones) Fractures of long bones Epiphyseal fractures and separations Subperiosteal new bone formation Digital fractures
Campomelic dysplasia	Hypoplastic vertebral bodies (thoracic vertebral pedicle absence) Hypoplastic scapulae 11 pair of ribs instead of 12 Narrow thorax (may be bell shaped) Scoliosis/kyphoscoliosis Short bowed humerus	Narrow iliac wings Poor pubis ossification Short bowed femur
Spondyloepiphyseal dysplasia congenita	Platypondyly (with maintained bone density) Pear shaped and bulbous vertebrae may be seen Kyphoscoliosis Intervertebral disc space is narrowed Delayed ossification of humeral epiphysis Bowing of humerus, short bone, early onset arthritis can be seen	Flat face Micrognathia Delayed ossification of pubis Bowing of femur can be seen
Achondroplasia	Marked symmetrical shortening of long bones particularly humerus Normal epiphysis with relative splaying and flaring involving metaphysis, may give ball and socket appearance Kyphoscoliosis Posterior scalloping of vertebral bodies Narrowing of spinal canal Height of discs nearly equal to vertebral body Short and thick pedicle Ulna often shorter than radius	Large cranial vault and small skull base Foramen magnum narrowing Short hand phalanges with trident-hand appearance Caudal narrowing of lumbar interpediculate distance Notch-like sacroiliac groove Decreased acetabular angles Small and square iliac wings (tombstone-shaped) Champagne glass shaped pelvic inlet Long fibulae

Table 1 (Continued)

Disease entity	Findings in CXR	Findings in other radiographs
Metaphyseal chondrodysplasia	Metaphyseal broadening and irregularities with preserved epiphysis Bulbous expansion of metaphysis (Jansen type)	
Cleidocranial dysostosis	Anomalous clavicular development (partly/ completely absent) Short and oblique ribs, may be supernumerary Delayed mineralization, hemivertebrae, spina bifida occulta and biconvex bodies may be found in spine (upper thoracic predominantly) Small, winged and elevated scapula Narrow/cone shaped chest (frequent) Kyphoscoliosis Shoulder dislocation may be seen	Wide-open sutures and patent fontanelles Wormian bones Depressed nasal bridge Hypertelorism Hypoplastic mid-facial region Prognathic mandible High arched palate Retention of deciduous teeth Delayed eruption of permanent dentition Short/absent radius may be seen Wide pubic symphysis Hypoplastic iliac wings Widened sacroiliac joints Large femoral neck with coxa vara Lengthening of the second metacarpal Hypoplastic pointed phalanges may be seen
Osteogenesis Imperfecta	Osteopenia Fractures (long bone diaphyses, apophyses and spine -most common site) Hyperplastic callus, Pseudoarthrosis, Deformities Ossification of interosseous membrane, popcorn calcification, dense metaphyseal bands Platyspondyly/codfish vertebra Spondylolysis and spondylolisthesis, kyphoscoliosis can be seen	Osteopenia Fractures Deformities [Prominent occipital region (Darth Vader appearance), Cranial vault flattening with transverse infolding of base (Tam O'Shanter skull), diaphyseal bending or angulation] Wormian bones

with postaxial polydactyly, disproportionate dwarfism (acromesomelia), congenital heart defects (ASD most common), nail, and teeth changes. Apart from short ribs,¹² one typical imaging finding is the outward bowing of the humerus along with short forearm bones¹³ (►Fig. 11).

Caffey's disease: It is a self-limiting disease usually presenting before 5 months of birth. Pathological hallmark is periosteal new bone formation with associated cortical thickening. The common clinical manifestation is classic triad including hyperirritability, soft tissue swelling, and hard mass over affected bones (most commonly involving mandible, clavicle, and ribs symmetrically). The imaging findings in CXR in Caffey's disease include thickened cortex and widened clavicle, cortical hyperostosis involving lateral ribs, unilateral involvement of scapula common (may be confused with malignancy), thick cortex involving diaphysis

of tubular bones, and sparing epiphysis (ulnar involvement more common; ►Fig. 12). Interosseous bridging can be seen in ribs and between radius and ulna.¹⁴ Vertebrae are spared. The close differential is child abuse, however symmetrical involvement of clavicle and ribs is seen in Caffey's disease.¹⁵

Other diseases having abnormal shapes of ribs include neurofibromatosis 1 (twisted ribbon ribs)¹⁶ and Melnick-Needles syndrome (wavy ribs with diaphyseal constrictions and curvature in long bones),¹⁷ among others (►Fig. 13).

Abnormality in the Thoracic Spine

Campomelic dysplasia: It is diagnosed antenatally commonly with key features including narrow thorax, bowed femur and

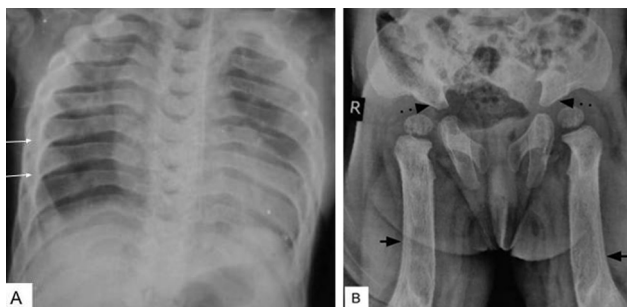


Fig. 3 (A,B) Mucopolidosis. CXR (A) shows uniformly widened ribs without increased density, pelvis and lower limb radiograph (B) shows widened undermodeled femora with periosteal thickening (arrows), note comma shaped iliac bones (dotted arrows).

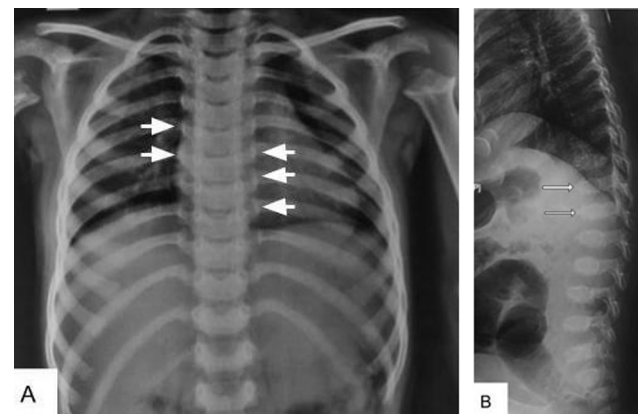


Fig. 4 (A,B) Pseudoachondroplasia. CXR (A) shows striking finding in the form of widening of costovertebral junctions (arrows), lateral radiograph of DL spine (B) shows anterior tongue like projection in the vertebral bodies (arrows).

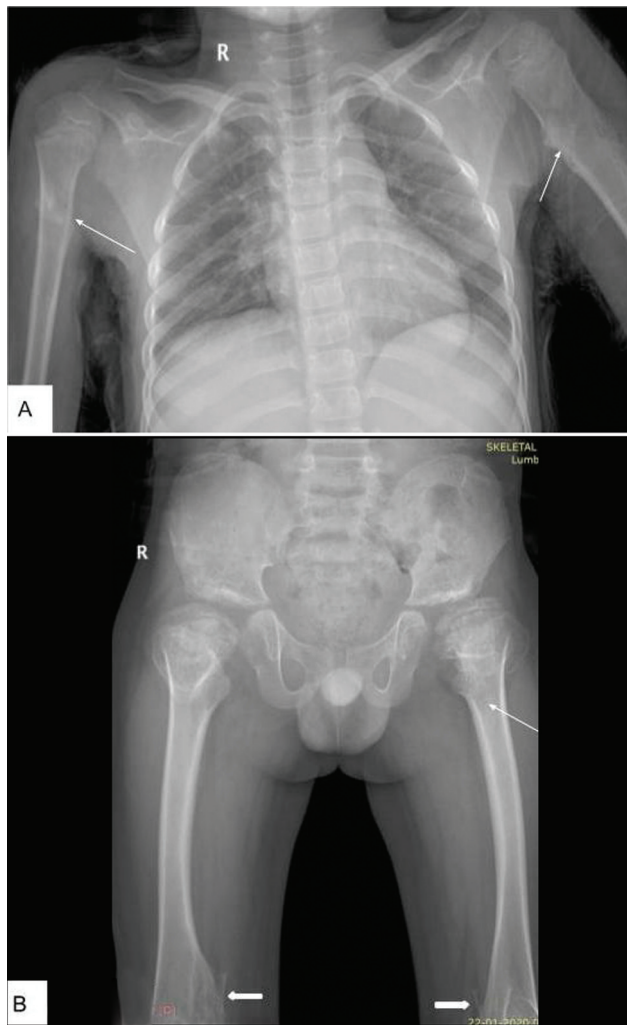


Fig. 5 (A,B) Hereditary Multiple Exostosis. CXR (A) shows broad based (sessile) osteochondroma affecting proximal humeri (arrows), pelvis and lower limb radiograph (B) shows osteochondroma arising from proximal metaphysis (long arrow) and pedunculated osteochondroma arising from distal metaphysis of bilateral femur (short arrows).

tibia, and hypoplastic scapulae. Imaging findings include the absence of thoracic vertebral pedicles. Other important features include hypoplastic scapulae, occasional short bowed upper limbs, and 11 pairs of ribs¹⁸ (► **Fig. 14**). Other imaging features are listed in ► **Table 1**.

Spondyloepiphyseal dysplasia congenita (SEDC): This is a form of collagenopathy, having clinical features secondary to multiple organ affection. CXR shows universal platyspondyly (more evident on a lateral view) with maintained bone density, kyphoscoliosis, and delayed ossification of humeral epiphysis.¹⁹ Secondary to the epiphyseal abnormality, early degenerative changes may be evident at multiple joints. Other imaging features are listed in ► **Table 1**.

Spondyloepiphyseal dysplasia tarda (SEDT): Many forms exist. Diagnostic imaging findings on a CXR include platyspondyly with posterior “heaping” of vertebral bodies (► **Fig. 15**). Visualized epiphyses show irregularity and early degenerative changes.²⁰

Chondrodysplasia punctate (CDP): It has an abnormal epiphyseal osseous nucleus and has two main forms, rhizo-



Fig. 6 (A,B,C) Enchondromatosis. CXR (A,B) Chest radiograph demonstrates lytic lesions in ribs with sharp margin clearly visualized in ribs (arrow), AP Knee (C) additionally shows multiple lytic lesions (arrow) involving distal metaphysis of femur and proximal metaphysis of tibia and fibula in the same patient, punctate foci of calcification (bent arrows) noted within.

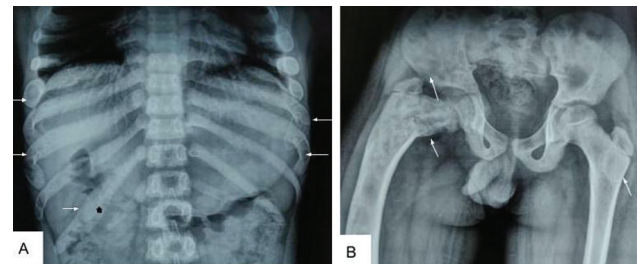


Fig. 7 (A,B) Polyostotic fibrous dysplasia. CXR (a) shows polyostotic smooth expansile lytic lesions within lateral ribs with rind sign (arrows) and ground glass matrix (asterisk), pelvis and lower limb radiograph (B) shows polyostotic lytic lesions within bilateral femur and ilium (arrows) with shepherd's crook deformity of right femur.

melic type (lethal) and Conradi–Hünemann variety (milder type). Imaging findings on a CXR include stippling of vertebral bodies (► **Fig. 16**), coronal clefting (lateral radiograph), kyphoscoliosis, and stippled epiphysis of the humerus. Short humeri are evident in the rhizomelic form.²¹

Spondylometaphyseal dysplasias (SMD): On a frontal CXR, the most prominent abnormalities lie in the long bone metaphyses²² (discussed later).

Long Bone (Humerus/Ulna) Abnormal

Achondroplasia: It is the most common cause of congenital dwarfism (rhizomelic) resulting from disturbance in *FGFR3* gene.²³ On a CXR, the most striking abnormality is a shortening of humeri (rhizomelic shortening).²⁴ The proximal

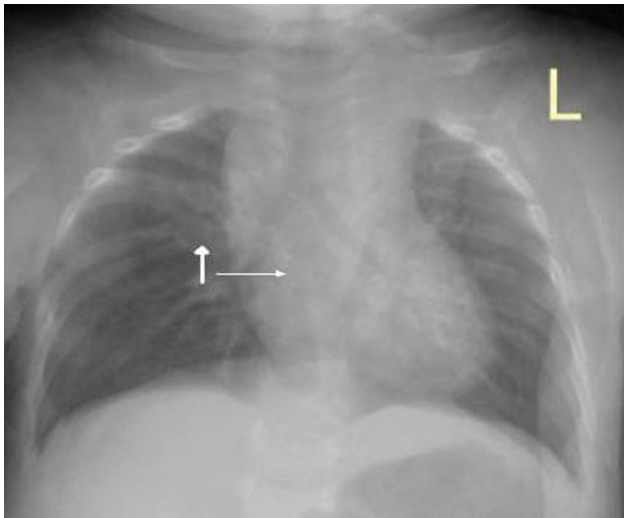


Fig. 8 Spondylocostal dysostosis. CXR shows vertebral segmentation anomalies spanning over 10 vertebral bodies (arrow) with abnormal fused ribs (short arrow).

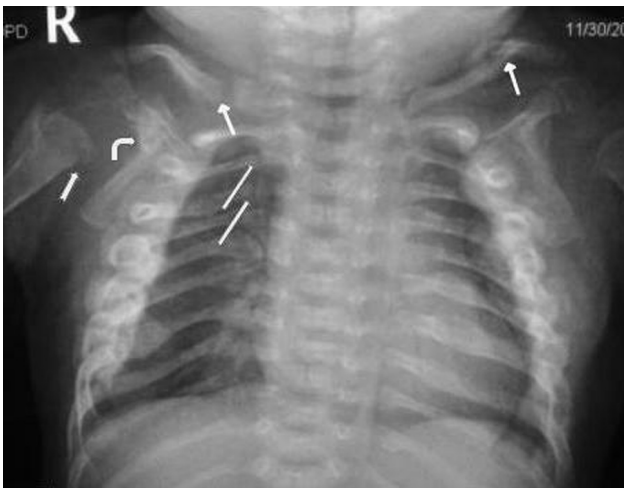


Fig. 9 Nonaccidental injury. The highly specific findings demonstrated are posterior rib fracture (long arrows), fracture of scapula (bent arrow), and metaphyseal fractures (notched arrow), also noted bilateral clavicular fractures (short arrows).

humeral metaphyses are flared, and the inferior angle of scapula are square in shape (►Fig. 17). On lateral CXR, several other imaging findings may be appreciated, namely, posterior scalloping of vertebral bodies, kyphoscoliosis, and short and thick pedicles²⁴. Other characteristic imaging findings are discussed in ►Table 1.²⁴

Metaphyseal chondrodysplasia (MCD): Several forms exist (e.g., Schmid, McKusick, and Jansen type). The common imaging finding evident on a frontal CXR is irregularity and broadening of proximal humeral metaphyses²⁵ (►Fig. 18). It is important to differentiate them from metabolic bone disease (rickets)²⁵ and spondylometaphyseal group of disorders. While rickets show reduced bone density, widening of growth plate, and widening of anterior rib ends, MCDs usually have normal bone density. A differentiation of MCD from SMD requires evaluation of a complete skeletal

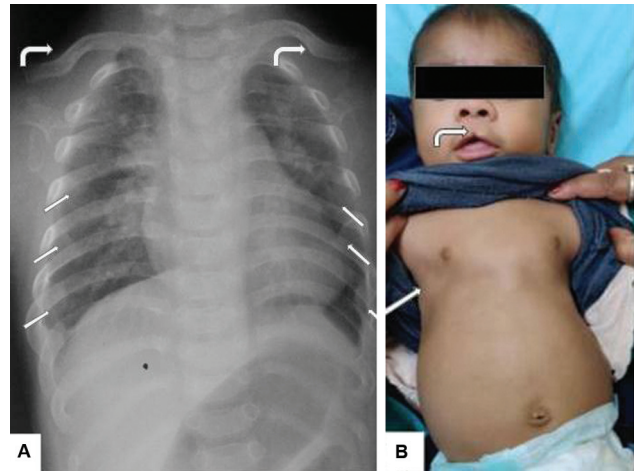


Fig. 10 (A,B) Juene's asphyxiating thoracic dystrophy (JATD). CXR (A) demonstrating narrow thorax and short ribs with small anterior segment (arrow); elevated clavicles (handle bar appearance) (bent arrow) is also seen in this case of Jeune syndrome. Child, clinical photograph (b) of the child with narrow thorax (arrow) and associated median cleft lip (bent arrow).

survey although a lateral CXR can also provide a clue about the shape and size of vertebrae. Differentiation between various types requires the analysis of patterns of metaphyseal involvement. Characteristic imaging findings are discussed in ►Table 1.

SMD: It is a heterogeneous group of disorders consisting of several different varieties; SMD is manifested on radiographs as a combination of metaphyseal and spinal abnormalities. The spinal manifestations vary, ranging from universal platyspondyly and medially located rounded pedicles (in Kozłowski subtype) to rounded vertebral bodies (in Sutcliffe subtype)²² (►Fig. 19).

SEDC and SEDT: These entities are discussed above in the section "Abnormality in the Thoracic Spine."

Non-accidental injury: This entity is mentioned above in the section "Abnormality in the Ribs."

Multiple epiphyseal dysplasia (MED): On a CXR, notable imaging findings of MED include delayed ossification of epiphysis with irregular flattened epiphysis, early osteoarthritic changes, and metaphyseal widening.²⁶

Metatropic dysplasia: This rare dysplasia is evidenced on a frontal CXR with rhizomelic shortening with prominent metaphyseal flaring (resembling dumbbell appearance) of the humeri²⁷ (►Fig. 20). Other features in chest radiograph include marked platyspondyly and kyphoscoliosis.²⁷

Diastrophic dysplasia: Clinical clues in this dysplasia include a deformed "Hitchhiker's thumb" and cauliflower ear. On a frontal CXR, imaging findings include shortened long bones with metaphyseal flaring.²⁸

Pseudoachondroplasia, MPS, EVC, HME, SEDC, and CDP also show abnormality in the long bones (discussed earlier).

Clavicle Abnormal

Cleidocranial dysostosis: It is characterized by defective ossification of membranous and enchondral bones (►Fig. 21). Diagnostic imaging finding is an anomalous



Fig. 11 (A,B) Ellis-van Creveld syndrome. CXR (A) shows narrow thorax with short ribs (arrow), short humerus with external bowing (bent arrow), visualized radius and ulna are also small (notched arrow), feet and hand radiograph (B) shows postaxial polydactyly.

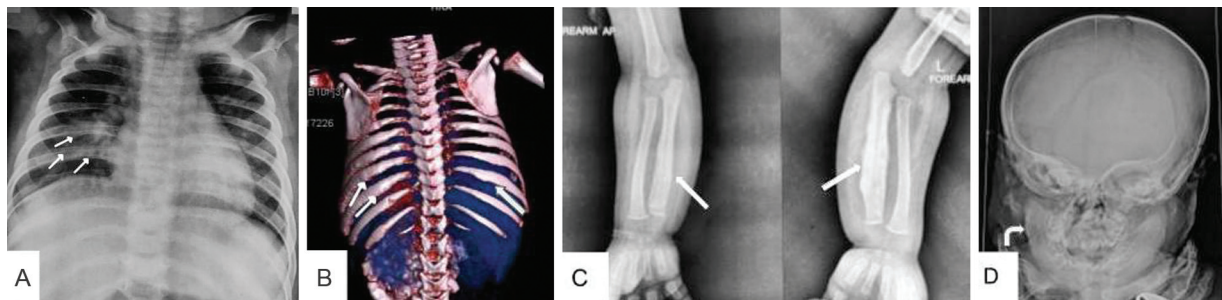


Fig. 12 (A–D) Caffey's disease in a 3 month old girl child presenting with fever and irritability, CXR (A) shows cortical thickening involving multiple ribs (arrow), CT volume rendering (B) shows cortical hyperostosis with widening involving multiple ribs (arrow). (C, D) Additionally shows thickened cortex involving diaphysis of b/l ulna with sparing of epiphysis (arrows), also observe hyperostosis of mandible (bent arrow).

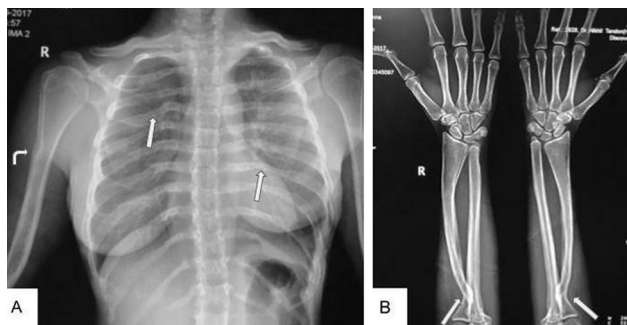


Fig. 13 (A,B) Melnick Needles syndrome/osteodysplasty. CXR (A) shows wavy ribs with cortical constriction (arrows), cortical constriction of right humerus is also noted (bent arrow), upper limb radiograph (B) shows curved bilateral radius with cortical constriction (arrows).

clavicular development (partly/completely absent). Other features in CXR include supernumerary ribs, short or oblique ribs, hemivertebrae, spina bifida occulta, biconvex bodies, and kyphoscoliosis (upper thoracic predominantly).²⁹ Other features are listed in **Table 1**.²⁹

Nonaccidental injury, MPS, JATD, and Caffey's disease also show abnormality in clavicles (discussed above).

Soft Tissue Abnormality

Fibrodysplasia ossificans progressiva: It involves progressive ossification of soft tissue (striated muscle, ligaments, tendon, fascia, and aponeuroses) with associated congenital micro-

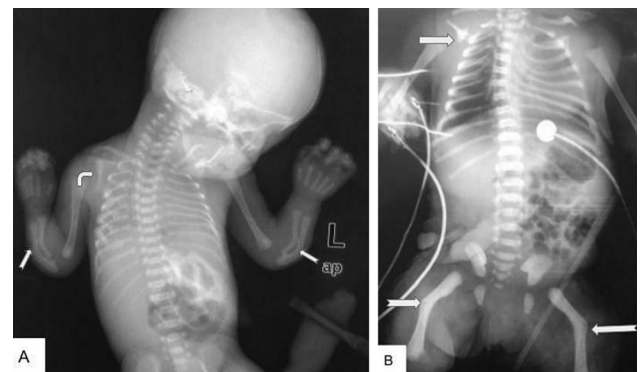


Fig. 14 (A,B) Campomelic dysplasia. Chest radiograph (A) shows narrow thorax (arrow) with small scapula (bent arrow). Also note bowing of radius and ulna (notched arrow). Another patient of Campomelic dysplasia. Infantogram (B) shows hypoplastic scapula (arrow) and bent femora (notched arrows).

dactyly of great toe, and hallux valgus. CXR may show sheet-like soft tissue ossification in the lateral chest wall, axilla, and neck (**Fig. 22**).³⁰ Secondary to these heterotopic ossifications, variable spinal deformities may ensue, eventually leading to restrictive lung disease and respiratory failure.³⁰

Calcinosis universalis: It is characterized by the diffusion of calcium deposition (extensive sheet like) in skin, subcutaneous tissue, tendons, or muscles.³¹

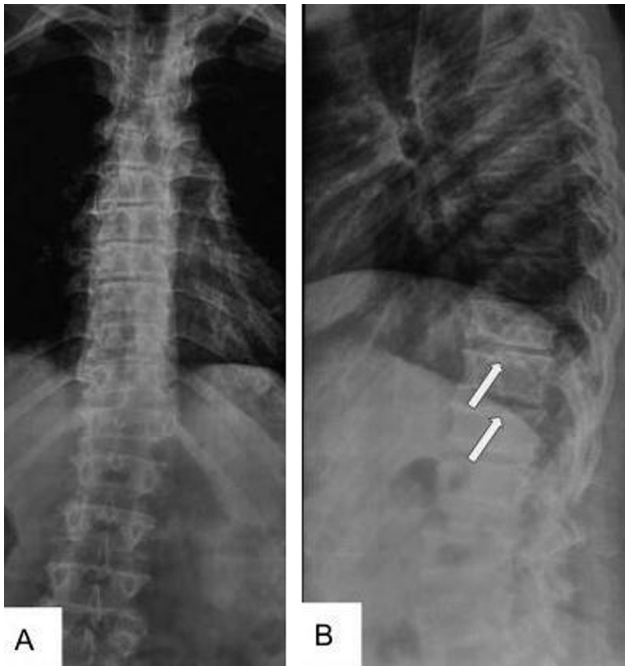


Fig. 15 (A,B) Spondyloepiphyseal dysplasia tarda. CXR frontal (A) and lateral view (B) show heaped up vertebrae posteriorly (arrow). In older age, platyspondyly can be seen.

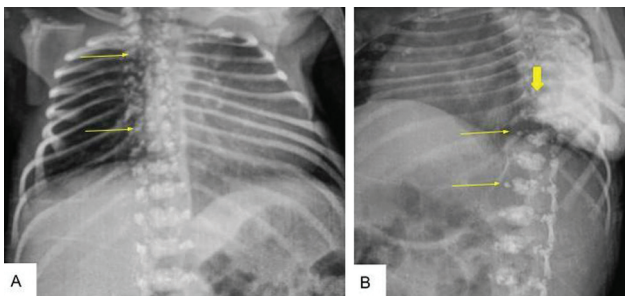


Fig. 16 (A,B) Chondrodysplasia punctata. CXR frontal (A) and lateral view (B) show stippling of vertebral bodies (arrows), coronal clefting is also noted in lateral view (short arrow).



Fig. 17 Achondroplasia. Chest radiograph showing short humeri (arrows) which should raise a suspicion of a cause of rhizomelic shortening.



Fig. 18 Metaphyseal chondrodysplasia. CXR shows metaphyseal irregularities involving right humerus with associated bulbous expansion (arrow) and preserved epiphysis (bent arrow), also there is shortening of humerus.



Fig. 19 (A,B) Spondylometaphyseal dysplasia (Kozlowski type). The striking finding in (A) is reduced vertebral height with medially placed pedicles (arrows), lateral radiograph of DL spine (B) shows reduced vertebral height with anterior tapering (bent arrows) and increased disk space, there were associated metaphyseal changes (not shown here); another differential on this CXR would have been SEDC.

Reduced Bone Density

Abnormality in Ribs and/or Thoracic Spine

Achondrogenesis: This lethal dysplasia is characterized by decreased bone mineralization, micromelia, short trunk, and macrocranium. On a CXR, the crucial imaging finding is poor ossification of vertebral bodies³² (nonvisualized vertebral bodies and only pedicles visualized). Other features in chest radiograph include shortened long bones (as a result of multiple intrauterine fractures) and thin ribs with/without fracture (fracture in Type 1A).³²

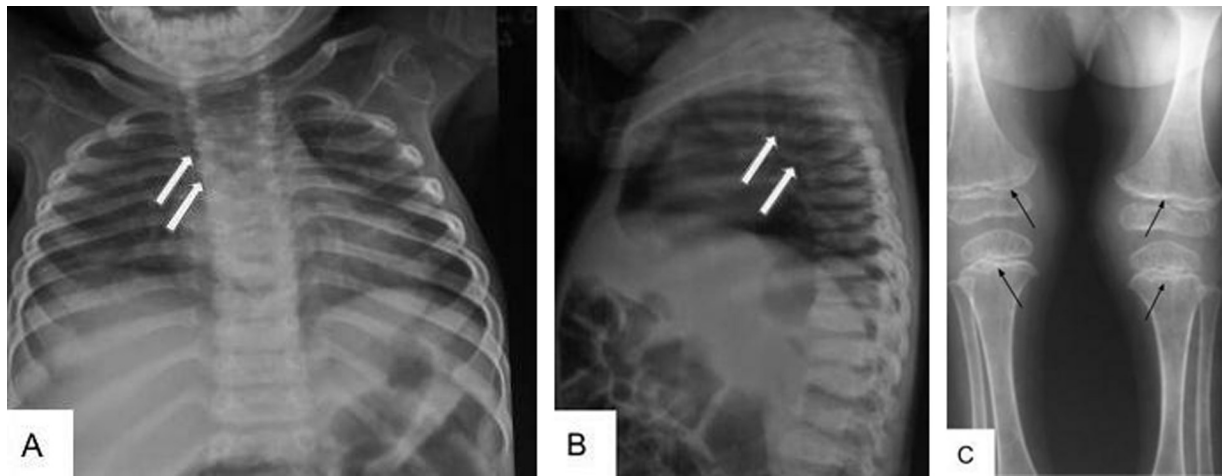


Fig. 20 (A,B,C) Metatropic dysplasia. CXR frontal (A) and lateral view (B) shows platyspondyly (arrows) and lower limb radiograph (C) shows small femur (rhizomelic shortening) with metaphyseal flaring involving distal femur and proximal tibia (arrows).

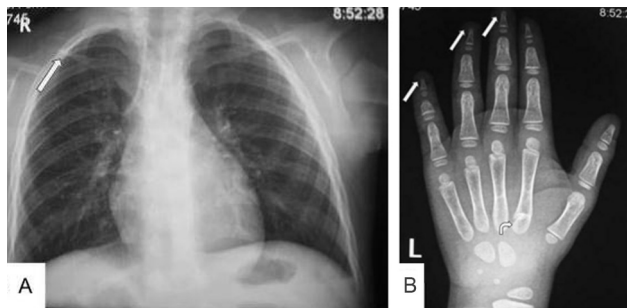


Fig. 21 (A,B) Cleidocranial dysostosis in a 5 year old boy. CXR (A) showing right clavicular hypoplasia (arrow), hand radiograph (B) showing distal tapering of distal phalanges (arrows), and additional epiphyseal center (bent arrow) at the base of second metacarpal; he also had pubic diastasis (not shown).



Fig. 22 Fibrodysplasia ossificans progressiva. Chest radiograph shows ectopic dense calcification in the form of column of bones around chest wall is noted bilaterally (arrow), also noted is opacity in left mid zone (bent arrow). Comment: Involvement of ribs and intercostal muscles can lead to restrictive lung disease and respiratory failure.

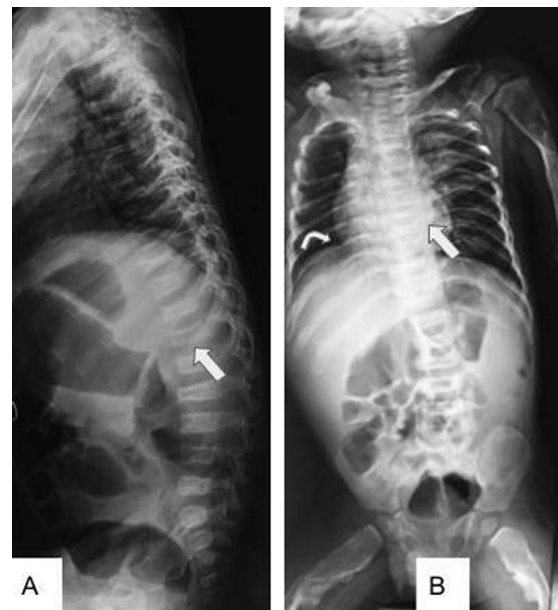


Fig. 23 (A,B) Osteogenesis Imperfecta. CXR lateral (A) and frontal view (B) shows platyspondyly (arrows), thin ribs (bent arrows). Note is made of deformed left humerus and both femora as a sequela of fracture.

Osteogenesis imperfecta (OI): It is characterized by reduced bone density with increased fragility due to abnormal type I collagen. It has different types of varying severity. Imaging findings include diffuse osteopenia, platyspondyly/codfish vertebra, thin ribs, and multiple fractures with/without hypertrophic callus formation³³ (►Fig. 23). Secondary to multiple repeated fractures, several deformities may be evident. Ossification of interosseous membrane is a typical imaging finding in type V OI. Popcorn calcification and dense metaphyseal bands can be seen.³³ Other characteristic imaging findings are discussed in ►Table 1.³³

Abnormality in Long Bones

Achondrogenesis: It is explained in “Reduced Bone Density” section.

OI: It is mentioned above



Fig. 24 Osteopetrosis with rickets. Note the increased densities involving all ribs, humerus, and vertebrae, obliterated medullary cavities. Rachitic changes are evident in the form of metaphyseal widening and irregularity.

Increased Bone Density

There are few skeletal dysplasias which present with diffuse increased bone density; however, increased bone density can be a normal finding in a neonatal CXR and needs to be meticulously evaluated.

Abnormality in the Ribs/Spine

Osteopetrosis: It is caused by defective osteoclastic resorption leading to abnormal bone maturation with the formation of dense and brittle bones. Severe cases are diagnosed in infancy with clinical features including anemia, hepatosplenomegaly, bleeding episodes, fractures, and failure to thrive. Diagnostic imaging pointers are sclerotic ribs with obliteration of medullary cavity, sclerotic clavicle, and humeri with “bone within bone” appearance, sandwich vertebrae on a lateral CXR, and evidence of repeated fractures³⁴ (→ **Fig. 24**).

Pyknodysostosis: This often comes as an imaging differential of osteopetrosis. It is characterized by osteosclerosis;

Table 2 Role of CXR in skeletal dysplasia diagnosis

Conditions where CXR alone may be sufficient	Conditions where CXR plays an important adjunct role
<ul style="list-style-type: none"> • Spondylocostal dysostosis • Short rib dysplasias • Ellis–van Creveld syndrome • Cleidocranial dysostosis • Osteogenesis imperfecta • Fibrodysplasia ossificans progressiva • Polyostotic fibrous dysplasia • Hereditary multiple exostoses 	<ul style="list-style-type: none"> • Osteopetrosis • Craniodiaphyseal dysplasias • Achondroplasia • Pseudoachondroplasia • Mucopolysaccharidosis • Polyostotic fibrous dysplasia • Enchondromatosis • Hereditary multiple exostoses • Epiphyseal dysplasias • Metaphyseal dysplasias

Abbreviation: CXR, chest X-ray.

Table 3 Conditions where CXR is diagnostic at birth

JATD SRPS Achondroplasia Osteogenesis imperfecta

Abbreviations: CXR, chest X-ray; JATD, Jeune’s asphyxiating thoracic dystrophy; SRPS, short-rib polydactyly syndromes.

however, medullary canal of long bones is preserved (versus osteopetrosis).³⁵ Dense vertebral bodies with sparing of the transverse processes and a typical “spool shape” are described. Other important associated findings are acro-osteolysis, wide open sutures, obtuse mandibular angle, etc.³⁶

Long Bone (Humerus/Ulna) Abnormal

Several other sclerosing bone dysplasias may present with sclerosis of long bones, namely, osteopathia striata, melorheostosis, progressive diaphyseal dysplasias, and craniodiaphyseal dysplasias (→ **Fig. 25**). While some (melorheostosis) may have characteristic imaging findings on a single CXR,³⁷ most of them require a full skeletal survey and clinical details to reach a diagnosis.

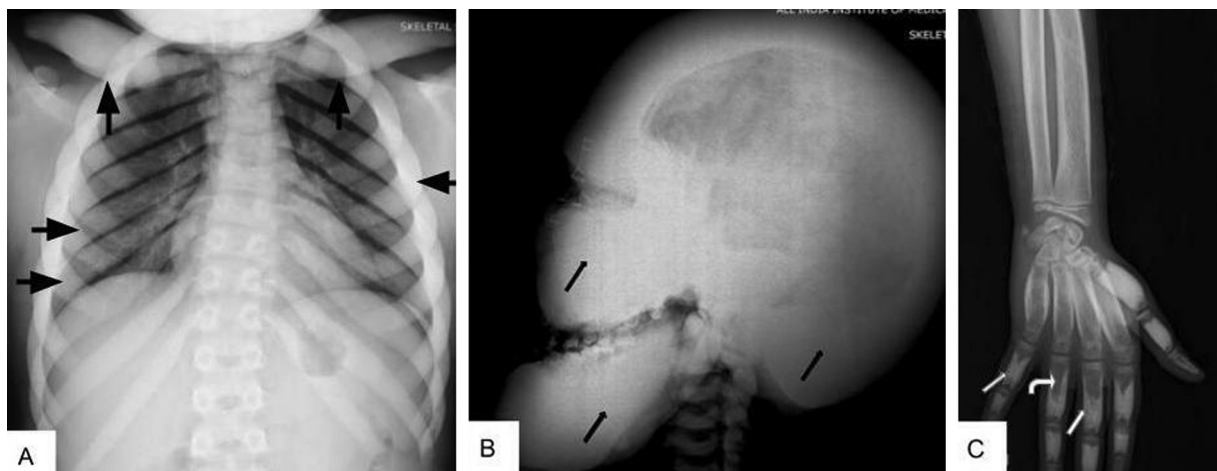


Fig. 25 (A,B,C) Craniodiaphyseal dysplasia in a 15 year boy, having no organomegaly or anemia. CXR (A) shows diffuse osteosclerosis (arrows) involving all visualized bones, mimicking osteopetrosis. However, lateral skull radiograph (B) reveals extreme bone sclerosis of facial and calvarial bones (arrows), hand radiograph (C) show diaphyseal sclerosis involving the phalanges and metacarpals (arrows); however, the medullary cavity (bent arrow) is maintained.

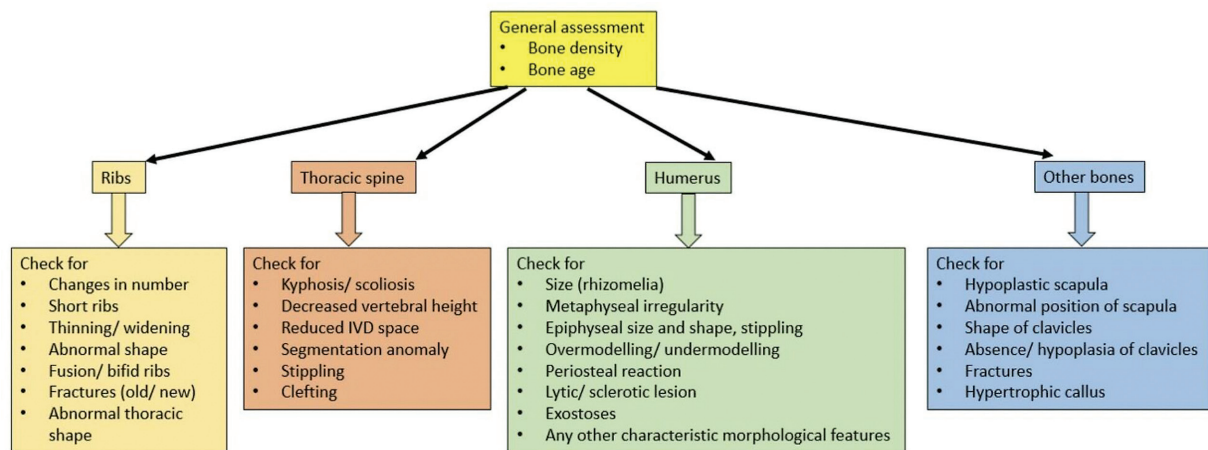


Fig. 26 Segment-wise approach. Segment-wise approach toward skeletal abnormalities in a CXR.

The Role of Chest X-Ray Alone in Making the Diagnosis

Most often, CXR is useful as a part of the whole skeletal survey. However, there are a few conditions where the diagnosis of the specific skeletal dysplasia/close differential can be reasonably accurately made on a CXR alone. These are listed in ►Table 2. There are few dysplasias where CXR is diagnostic at birth as listed in ►Table 3.

Conclusion

Skeletal dysplasia is not a single-film imaging diagnosis. It requires evaluation of the complete skeletal survey, along with appropriate clinical details. However, often the CXR may be the first imaging clue to an unsuspecting case, being evaluated for unrelated causes. Hence, radiologists should be aware of the various subtle and overt imaging findings of different dysplasias on a CXR. Segment-wise approach toward skeletal abnormalities in a CXR is given in ►Fig. 26.

Availability of Data and Material
Data available on request.

Contribution of Authors

R.J. contributed to data collection, literature review, and analysis and drafted the manuscript and critical revision. P.N. contributed to data collection, literature review, and analysis and drafted the manuscript and critical revision. N.G. contributed to data collection, literature review, analysis, and critical revision. P.S. contributed to data collection, literature review, and analysis and drafted the manuscript. M.K. contributed to data collection, literature review, analysis, and critical revision. A.K.G. contributed to data collection, literature review, analysis, and critical revision. M.J. contributed to data collection, literature review, and analysis and drafted the manuscript and critical revision.

Funding
None.

Conflict of Interest
None declared.

Declaration of Patient Consent

The authors certify that they have obtained all appropriate patient consent forms. In the form, the patient(s) has/have given his/her/their consent for his/her/their images and other clinical information to be reported in the journal. The patients understand that their names and initials will not be published and due efforts will be made to conceal their identity but anonymity cannot be guaranteed.

References

- 1 Mortier GR, Cohn DH, Cormier-Daire V, et al. Nosology and classification of genetic skeletal disorders: 2019 revision. *Am J Med Genet A* 2019;179(12):2393–2419
- 2 Palmucci S, Attinà G, Lanza ML, et al. Imaging findings of mucopolysaccharidoses: a pictorial review. *Insights Imag* 2013;4(04):443–459
- 3 Lai LM, Lachman RS. Early characteristic radiographic changes in mucopolipidosis II. *Pediatr Radiol* 2016;46(12):1713–1720
- 4 Tandon A, Bhargava SK, Goel S, Bhatt S. Pseudoachondroplasia: a rare cause of rhizomelic dwarfism. *Indian J Orthop* 2008;42(04):477–479
- 5 Murphey MD, Choi JJ, Kransdorf MJ, Flemming DJ, Gannon FH. Imaging of osteochondroma: variants and complications with radiologic-pathologic correlation. *Radiographics* 2000;20(05):1407–1434
- 6 Park Y-K. Multiple enchondromatosis (Ollier's Disease). In: Santini-Araujo E, Kalil RK, Bertoni F, Park Y-K, eds. *Tumors and Tumor-Like Lesions of Bone: For Surgical Pathologists, Orthopedic Surgeons and Radiologists*. London: Springer; 2015:253–258
- 7 Kushchayeva YS, Kushchayev SV, Glushko TY, et al. Fibrous dysplasia for radiologists: beyond ground glass bone matrix. *Insights Imag* 2018;9(06):1035–1056
- 8 Turnpenny PD, Sloman M, Dunwoodie S. ICVS (International Consortium for Vertebral Anomalies and Scoliosis). Spondylocostal Dysostosis, Autosomal Recessive. In: Adam MP, Ardinger HH,

- Pagon RA, Wallace SE, Bean LJ, Stephens K, et al., eds. GeneReviews® [Internet]. Seattle, WA: University of Washington; 1993 [cited 2020 Dec 20].
- 9 Dwek JR. The radiographic approach to child abuse. *Clin Orthop Relat Res* 2011;469(03):776–789
 - 10 Handa A, Voss U, Hammarsjö A, Grigelioniene G, Nishimura G. Skeletal ciliopathies: a pattern recognition approach. *Jpn J Radiol* 2020;38(03):193–206
 - 11 de Vries J, Yntema JL, van Die CE, Crama N, Cornelissen EAM, Hamel BCJ. Jeune syndrome: description of 13 cases and a proposal for follow-up protocol. *Eur J Pediatr* 2010;169(01):77–88
 - 12 Popli MB, Popli V. Ellis-van Creveld syndrome. *Indian J Radiol Imaging* 2002;12(04):549–550
 - 13 Ohashi I, Enomoto Y, Naruto T, et al. A severe form of Ellis-van Creveld syndrome caused by novel mutations in *EVC2*. *Hum Genome Var* 2019;6:40
 - 14 Phatak SV, Kolwadkar PK, Phatak MS. Pictorial essay: infantile cortical hyperostosis (Caffey's disease). *Indian J Radiol Imaging* 2004;14(02):185–186
 - 15 Yochum TR, Rowe LJ. Yochum and Rowe's Essentials of Skeletal Radiology. 3rd ed. Philadelphia: Lippincott/Williams & Wilkins; 2005
 - 16 Glass RBJ, Norton KI, Mitre SA, Kang E. Pediatric ribs: a spectrum of abnormalities. *Radiographics* 2002;22(01):87–104
 - 17 Oh CH, Lee CH, Kim SY, Lee S-Y, Jun HH, Lee S. A family of Melnick-Needles syndrome: a case report. *BMC Pediatr* 2020;20(01):1–6
 - 18 Kaissi AA, van Egmond-Fröhlich A, Ryabykh S, et al. Spine malformation complex in 3 diverse syndromic entities: case reports. *Medicine (Baltimore)* 2016;95(50):e5505
 - 19 Themes UFO. Spondyloepiphyseal Dysplasia Congenita. 2020 [cited 20 Dec 2020]. Accessed November 29, 2022 at: <https://radiologykey.com/spondyloepiphyseal-dysplasia-congenita/>
 - 20 Lakhkar BN, Raphael R. Spondyloepiphyseal dysplasia: an evaluation of six cases. *Indian J Radiol Imaging* 2003;13:199–202
 - 21 Morthy NL, Venkataratnam I, Rao RP, Rani MS. Images: Chondrodysplasia punctata. *Indian J Radiol Imaging* 2002;12(03):397–398
 - 22 Duarte ML, Duarte ÉR, Solorzano DB, Solorzano EB, Ferreira Jde ASpondylometaphyseal dysplasia: an uncommon disease. *Radiol Bras* 2017;50(01):63–63
 - 23 Aviezer D, Golembo M, Yayon A. Fibroblast growth factor receptor-3 as a therapeutic target for achondroplasia—genetic short limbed dwarfism. *Curr Drug Targets* 2003;4(05):353–365
 - 24 Sargar KM, Singh AK, Kao SC. Imaging of skeletal disorders caused by fibroblast growth factor receptor gene mutations. *Radiographics* 2017;37(06):1813–1830
 - 25 Pediatrics - OrthobulletsMetaphyseal Chondrodysplasia - Pediatrics - Orthobullets. 2020 [cited 2020 Nov 28]. Accessed November 29, 2022 at: <https://www.orthobullets.com/pediatrics/4099/metaphyseal-chondrodysplasia>
 - 26 Yadav P, Narula M. Dysplasia epiphysealis multiplex. *Indian J Radiol Imaging* 2000;10:267–268
 - 27 Kannu P, Aftimos S, Mayne V, Donnan L, Savarirayan R. Metatropic dysplasia: clinical and radiographic findings in 11 patients demonstrating long-term natural history. *Am J Med Genet A* 2007;143A(21):2512–2522
 - 28 Bonafé L, Mittaz-Crettol L, Ballhausen D, Superti-Furga A. Diastrophic dysplasia. In: Adam MP, Ardinger HH, Pagon RA, Wallace SE, Bean LJ, Stephens K, et al., eds. GeneReviews® [Internet]. Seattle, WA: University of Washington; 1993 [cited 2020 Dec 20].
 - 29 Patil PP, Barpande SR, Bhavthankar JD, Humbe JG. Cleidocranial dysplasia: a clinico-radiographic spectrum with differential diagnosis. *J Orthop Case Rep* 2015;5(02):21–24
 - 30 Al-Salmi I, Raniga S, Hadidi AA. Fibrodysplasia ossificans progressiva—radiological findings: a case report. *Oman Med J* 2014;29(05):368–370
 - 31 Hwang Z-A, Suh KJ, Chen D, Chan WP, Wu JS. Imaging features of soft-tissue calcifications and related diseases: a systematic approach. *Korean J Radiol* 2018;19(06):1147–1160
 - 32 Hattapoğlu S, Durmaz MS. Radiological features of achondrogenesis type 1A: case report and review of the literature. *Med J Obstet Gynecol* 2018;6(01):1115–1118
 - 33 Renaud A, Aucourt J, Weill J, et al. Radiographic features of osteogenesis imperfecta. *Insights Imaging* 2013;4(04):417–429
 - 34 Gangadhar SR, Prakashchandra SP, Rupal P. Osteopetrosis with typical radiological findings. Rare case report. *Int J Anatomy, Radiol Surg* 2015;4:36–38
 - 35 Ihde LL, Forrester DM, Gottsegen CJ, et al. Sclerosing bone dysplasias: review and differentiation from other causes of osteosclerosis. *Radiographics* 2011;31(07):1865–1882
 - 36 Pawar SS, Bhorge V. Pyknodystosis. *Indian J Radiol Imaging* 2001;11(03):151–151
 - 37 Boulet C, Madani H, Lenchik L, et al. Sclerosing bone dysplasias: genetic, clinical and radiology update of hereditary and non-hereditary disorders. *Br J Radiol* 2016;89(1062):20150349